Design of electrified fluidized bed calciner for direct capture of CO_2 from cement raw meal

Ladan Samaei*, Lars-Andre Tokheim, Christoffer Moen*****

** Department of Process, Energy and Environmental Technology, University of South-Eastern Norway (e-mail: 258911@usn.no)*

*** Department of Process, Energy and Environmental Technology, University of South-Eastern Norway (e-mail: Lars.A.Tokheim@usn.no)*

**** Heidelberg Materials Norway (e-mail: christoffer.moen@heidelbergmaterials.com)*

Abstract: In this study, a fluidized bed electrified calciner was designed, and various operating conditions were investigated by CPFD simulations. It was found that maintaining a constant fluidization velocity while increasing the temperature of hot cylinders or preheating the raw meal significantly enhances the calcination degree. Altering the fluidization velocity while keeping temperatures constant also greatly affects the calcination degree and particle entrainment. A fluidization velocity of 0.3 m/s appears to be optimal for the reactor, whereas 0.8 m/s resulted in complete entrainment of the bed. The maximum calcination degree achieved was 90% with preheated meal. The average meal residence time was found to be 24-26 s.

Keywords: CO_2 capture, Electrification, Fluidized bed, Calciner, CPFD

1. INTRODUCTION

With an estimated 2600 million tons of CO_2 emissions in 2020, the cement industry holds the second-largest share of direct industrial CO_2 emissions worldwide (IEA, 2020) Furthermore, because of urbanization and the growing global population, cement production is predicted to increase by 12–23% by 2050 (IEA., 2018). By 2050, the European Union (EU) wants to cut its greenhouse gas emissions by 80–95% from 1990 levels (Dupont and Oberthür, 2015). Achieving this objective will largely depend on decarbonizing the cement sector. About two thirds of the CO_2 emissions from the cement industry are from calcination of limestone, whereas one third comes from the burning of fuels (Nikolakopoulos et al., 2024). However, using green electricity to calcine the raw materials and combining this with storage of the pure CO_2 generated in the calcination process can vary significantly reduce CO_2 emissions in the cement industry (Tokheim et al., 2019).

By switching from fuel combustion to electrical energy for the cement process both in calciner and in the rotary kiln, two things happen at once. Firstly, the CO_2 produced from burning fuel in the calciner is eliminated, reducing the overall CO_2 emissions from making clinker. Secondly, the exhaust gas from the calciner is almost pure CO_2, so it can go straight to a CO_2 processing unit without needing a separate CO_2 separation plant. Having said that, if only the calciner uses the clean electricity instead of burning fuels while the kiln still uses the fuel combustion for providing heat, a significant reduction (around 70%) in emissions can be achieved. This happens while only one of the main equipment units in the kiln system (the calciner) needs to be altered. (Tokheim et al., 2019). An illustration of such a concept is shown in Fig. 1.

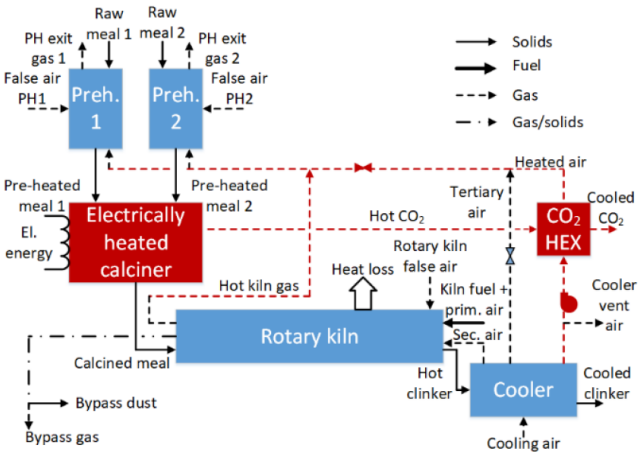

Fig. 1. Block flow diagram of a cement kiln system with electrified calciner (Tokheim et al., 2019).

Insisting on the benefits of using an electrified calciner, the question is which type of reactor is the best for designing an electrified calciner? This has been investigated in previous studies, and a fluidized bed (FB) calciner was found to be a good candidate as it provides good mixing and high heat and mass transfer (Samani et al., 2020). The raw meal feed is usually a fine powder (median size less than 30 µm) which can be classified as Geldart C particles. Geldart C particles are difficult to fluidize due to large inter-particle forces in comparison with the drag forces applied by the gas (Geldart, 1973). One way to tackle this problem is to improve the fluidization properties by mixing the small particles with coarse inert particles. After calcination of the meal, separation and entrainment of Geldart C particles is obtained by a change in the gas velocity. The reactor should be designed in such a way that the coarse particles remain in the bed, whereas the fine uncalcined particles are continuously fed close to the

bottom of the bed and fine calcined particles are continuously discharged at top of the bed. The CO_2 evolving from the calcination reaction will contribute in the entrainment of the calcined particles.

The FB operating with a binary particle mixture has previously been studied in in several publications. Kato et al. (1991) investigated the residence time distribution of fine particles in a powder-particle FB. In another study, Tashimo et al. (1999) investigated the calcination of fine powder raw meal (Geldart C) in a powder-particle FB experimentally. Other studies and experiments have also been conducted in investigation of the fluidization conditions of binary particles FB (Kim et al., 2014). More recently a study was conducted by Jacob et al. (2022), who made an experimental and numerical investigation of using coarse particles for fluidization of fine limestone in the calciner. That study found that a fluidization velocity of 0.3 m/s and a weight fraction of 25 % fine particles gave a stable bed (Jacob et al., 2022).

A recent study by Jacob and Tokheim (2023) designed an electrified calciner with vertical heating channels and investigated this by CPFD simulations. While the designed calciner in that study showed promising results, in the industry it may be difficult to distribute the meal evenly between the heating channels, and therefore, there may be a risk that local overheating may occur.

The current study investigates an alternative heater arrangement, in the form of horizontally immersed cylindrical heating elements, as this will likely not prevent transverse mixing of the raw meal. A lab-scale electrified unit of about 100 kW is designed and simulated using the commercial CPFD software Barracuda. The main aims are to determine conditions for obtaining both fluidization, calcination, and separation in the designed reactor. Key process parameters, such as heater temperature, fluidization velocity and meal temperature are varied in different simulation cases.

2. METHODS

2.1 Design and sizing

A binary particle FB reactor with electrically heated immersed horizontal cylinders should be designed. A heat and mass balance is made, and FB calculations are performed to ensure good mixing and entrainment of fine calcined particles while keeping other particles in the bed. A trial-and-error procedure is required to find an appropriate size for the reactor and cylinders as well as an appropriate cylinder arrangement. The design calculations are done based on the assumption that the bottom cross section of the reactor is rectangular, and the length of the cylinders are all the same equal to one side of the bottom cross section. This assumption is needed because the cylinders should be electrically heated. Also, it is assumed that the reactor wall temperature is constant and that there is no heat loss.

The decomposition of calcium carbonate ($CaCO_3 \rightarrow CaO + CO_2$) is an endothermic reaction requiring 1.7 $\frac{MJ}{kg_{CaCO_3}}$ (Jacob, 2023). Also, the raw meal should be heated up to reach the calcination temperature (T_{cal}) before the reaction happens. Equation (1) shows the energy balance of the reactor where the first part shows the heat needed for the reaction and the second part shows the sensible heat needed to heat up the meal. In the equation, $\dot{m}_{rm}$, w_{CaCO_3} and C_{rm} are the mass flow rate of feeding raw meal to the reactor, the weight fraction of limestone in the raw meal and the specific heat capacity of the raw meal, respectively. η is the degree of calcination, H_{cal} is the enthalpy of calcination and $\dot{E}$ is the electric energy supply.

$$\dot{m}_{rm} w_{CaCO_3} \eta H_{cal} + \dot{m}_{rm} C_{rm} (T_{cal} - T_{in}) = \dot{E} \quad (1)$$

Using the energy balance, the mass flow rate of the raw meal is calculated. So, the required heat transfer area for the calcination and for heating up the meal can be calculated using (2) and (3), respectively. In both equations, U is the overall heat transfer coefficient which is assumed to be 0.3 $\frac{kW}{m^2K}$. ΔT in (2) shows the temperature difference between the hot cylinder wall and the calcination temperature, whereas ΔT_{LMTD} in (3) is the logarithmic mean temperature between the cylinder wall and the raw meal being heated.

$$A_{cal} U \Delta T = \dot{m}_{rm} w_{CaCO_3} \eta H_{cal} \quad (2)$$

$$A_{sensible} U \Delta T_{LMTD} = \dot{m}_{rm} C_{rm} (T_{cal} - T_{in}) \quad (3)$$

The overall heat transfer area is the sum of the areas in the equations above and is used to calculate the number of cylinders. This will be calculated after some trial-and-error procedure for defining the size of the bottom cross section of the reactor.

The procedure begins with the assumption of two values, L1 and L2, for the rectangular bottom cross section of the reactor, aiming to keep the area as small as possible. The mass of gas required to achieve the fluidization velocity is then calculated using (4) where u_F is the fluidization velocity. The produced CO_2 is calculated based on a mass balance (5)-(8), where M shows the molecular weight, and $\dot{m}$ and $\dot{n}$ show the mass flow rate and molar flow rate, respectively.

$$\dot{m}_{CO_2,inj} = \rho_{CO_2} u_F (L_1 L_2) \quad (4)$$

$$\dot{m}_{CaCO_3} = \dot{m}_{rm} w_{CaCO_3} \quad (5)$$

$$\dot{n}_{CaCO_3} = \frac{\dot{m}_{CaCO_3}}{M_{CaCO_3}} \quad (6)$$

$$\dot{n}_{CaCO_3} = \dot{n}_{CO_2} \quad (7)$$

$$\dot{m}_{CO_2,prod} = \dot{n}_{CO_2,prod} M_{CO_2} \quad (8)$$

The total CO_2, i.e., the sum of the injected and produced CO_2, determines the outlet velocity. If this velocity is below the required entrainment velocity, the calculation is repeated. As a design constraint the exit is cylindrical with a fixed diameter.

$$\dot{m}_{CO_2,out} = \dot{m}_{CO_2,inj} + \dot{m}_{CO_2,prod} \quad (9)$$

$$u_{out,CO_2} = \frac{\dot{m}_{CO_2,out}}{A_{top} \rho_{CO2}} \quad (10)$$

Next, the length of each hot cylinder is set to L_1, and the surface area for one cylinder is computed. Dividing the total heat transfer area ($A_{cal} + A_{sensible}$) by the surface area of one cylinder ($\pi D_{cyl} L_1$) gives the number of cylinders. The number of rows of cylinders needed are calculated. The height of the area including cylinders should be almost equal to the height of the bed. Adjustments are made to the cross-section dimensions until the desired conditions are met. Finally, the total reactor height is ensured to be adequate to retain coarse particles but short enough for proper calcination and entrainment of fine particles.

2.2 CPFD Simulation

Barracuda version 21.1.1 is used for the CPFD simulations. The simulation is conducted to investigate different operational conditions. The investigated operating conditions include variation in the temperature of the raw meal feed to the reactor, the wall temperature of the hot cylinders and the fluidization gas velocity. The reaction rate, amount of particle entrainment, entrainment velocity and pressure drop in the reactor are then compared for different simulation cases.

To do the simulations, after preparing the geometry and a proper grid the governing equations should be solved for the fluid and particle phases. Barracuda technology uses the 3D Multiphase Particle-in-Cell (3D-MP-PIC) method developed by CPFD Software. The MP-PIC method solves equations for both the gas and solids phases. It uses a Eulerian approach for the gas and a mix of the Eulerian and Lagrangian approach for the solids. Instead of tracking each physical particle, it groups similar ones into numerical parcels. This makes calculating properties like particle stresses faster in the gas phase. The method can handle various particle phases, sizes, and materials efficiently (Snider, 2001), (Jacob, 2023).

To define the fluid behavior in a CPFD simulation, equations for continuity, momentum, energy and species transport should be solved. In the continuity equation (11), θ_f, ρ_f and u_f are volume fraction, density and velocity of the fluid. Equation (12) shows the momentum equation where ∇p denotes the pressure gradient in the gas flow, τ_f symbolizes the stress exerted by the fluid, F is the inter-phase momentum transfer rate per unit, and g represents the gravity constant. Equation (13) is the species transport equation, where $Y_{f,i}$ and $\delta\dot{m}_{i,chem}$ are the mass fraction of species i in the fluid and the chemical source term, respectively. The term D_t is the turbulent mass diffusivity, which can be related to the flow viscosity by the Schmidt number correlation ($Sc = \frac{\mu}{\rho D}$). For a non-isothermal simulation, the energy equation (14) should also be solved. H_f is the enthalpy of the fluid, ϕ is the viscous dissipation rate, $\dot{q}_f''$ is the fluid heat flux, $\dot{Q}$ represents the energy source and S_h is the energy exchange between fluid and particles (Snider et al., 2011), (Jacob, 2023).

$$\frac{\partial(\theta_f \rho_f)}{\partial t} + \nabla \cdot \left(\theta_f u_f \rho_f\right) = \delta\dot{m}_p \tag{11}$$

$$\frac{\partial(\theta_f \rho_f u_f)}{\partial t} + \nabla \cdot \left(\theta_f \rho_f u_f u_f\right) = -\nabla p + F + \theta_f \rho_f g + \nabla \cdot \left(\theta_f \tau_f\right) \tag{12}$$

$$\frac{\partial(\theta_f \rho_f Y_{f,i})}{\partial t} + \nabla \cdot \left(\theta_f u_f \rho_f Y_{f,i}\right) = \nabla \cdot \left(\rho_f D_t \theta_f \nabla Y_{f,i}\right) + \delta\dot{m}_{i,chem} \tag{13}$$

$$\frac{\partial(\theta_f \rho_f H_f)}{\partial t} + \nabla \cdot \left(\theta_f \rho_f H_f u_f\right) = \theta_f \left(\frac{\partial p}{\partial t} + u_f \nabla p\right) + \phi - \nabla \cdot \left(\theta_f \dot{q}_f''\right) + \dot{Q} + S_h + \dot{q}_D + \dot{q}_w \tag{14}$$

Following the particle movement equation the term $\delta\dot{m}_p$ in the fluid continuity equation can be calculated in (15), where $\frac{dm_p}{dt}$ is the rate of change of the particle mass producing gas through chemistry and f is a function for particle movement, which depends on the particle spatial location x_p, velocity u_p, mass m_p, temperature T_p and time t. The particle volume fraction is defined in (16), which can also be used for calculating fluid volume fraction (θ_f) as the sum of particle volume fraction and fluid volume fraction is one. The particle acceleration is calculated using (17), where ρ_p is the particle density, D_p is the drag function, τ_p is the particle contact stress and τ_D is the particle collision damping time (Snider et al., 2011), (Jacob, 2023). The drag function selected for the simulations is the Wen-Yu/Ergun model, which is a blend of two drag models from Wen-Yu and Ergun. The former is more appropriate for dilute flows, while the latter works better for dense flows (Jacob and Tokheim, 2023). The energy equation for the particle lumped heat transfer assumes that the temperature within a particle has no spatial gradients, further, there is no heat release from chemical reactions inside the particles, and any heat released from reactions on the particle surface does not significantly affect the surface energy balance shown in (18), where C_v is the particle specific heat capacity, λ_f is the fluid thermal conductivity, Nu_{f-p} represents the Nusselt number of heat transfer between particle and fluid and A_{sp} is the particle surface area (Snider et al., 2011), (Jacob, 2023).

$$\delta\dot{m}_p = -\iiint f \frac{dm_p}{dt} dm_p du_p dT_p \tag{15}$$

$$\theta_p = -\iiint f \frac{m_p}{\rho_p} dm_p du_p dT_p \tag{16}$$

$$\frac{du_p}{dp} = D_p\left(u_f - u_p\right) - \frac{1}{\rho_p}\nabla p - \frac{1}{\theta_p \rho_p}\nabla \tau_p + g + \frac{\overline{u_p} - u_p}{\tau_D} \tag{17}$$

$$C_v \frac{dT_p}{dt} = \frac{1}{m_p}\frac{\lambda_f N u_{f-p}}{2 r_p} A_{sp}\left(T_f - T_p\right) \tag{18}$$

Considering the heat transfer between fluid and particles, in CPFD simulation the heat transfer coefficient between the two phases can be calculated in (19) Where *Re* and *Pr* are the Reynolds and Prandtl number, respectively, k_f is the fluid thermal conductivity and d_p is the particle diameter.

$$h_p = \left(0.37 Re^{0.6} \overset{0.33}{\Pr} + 0.1\right)\frac{k_f}{d_p} \tag{19}$$

The heat transfer between the fluid and the wall assuming isothermal wall can be calculated in (20) Where h_{fw} shows the heat transfer coefficient between fluid and wall, h_l is the lean gas phase heat transfer coefficient and h_d represents the dense particle phase heat transfer coefficient. It is noted that f_d, which shows the fraction of contact time by the dense particle phase, depends on the particle volume fraction at the wall, θ_p,

and the close pack value fraction, θ_{cp}. (Barracuda-Virtual-Reactor, 2022).

$$h_{fw} = h_l + f_d h_d \tag{20}$$

The radiation heat transfer from hot walls to the particles, which is calculated using "near wall model", is shown in (21), (22), where T_w and T_p are the temperature of the wall and the particle, respectively. σ is the Stefan-Boltzmann constant, ε_{wp} is the (volume averaged) particle emissivity, F_{wp} represents the wall-particle view factor and A_w is the wall area (Barracuda-Virtual-Reactor, 2022).

$$q_{wp} = A_w F_{wp} \varepsilon_{wp} \sigma \left(T_w^4 - T_p^4\right) \tag{21}$$

$$\varepsilon_{wp} = \left(\frac{1}{\varepsilon_p} + \frac{1}{\varepsilon_w} - 1\right)^{-1} \tag{22}$$

The only reaction in this reactor is the $CaCO_3$ decomposition ($CaCO_3 \rightarrow CaO + CO_2$). Equations (23) to (25) show the reaction kinetics. In (23), $\frac{dm_j}{dt}$ represents the rate of decomposition or formation of each component j within the meal, M_j denotes the molecular mass of component j, while ϑ_j signifies the stoichiometric coefficient related to the calcination reaction. p_{CO_2} stands for the partial pressure of CO_2 present in the calciner, A_{sp} represents the surface area of the meal particles, and A_{eff} denotes the excess area fraction, accounting for voids present within the particles. k_D is the rate kinetics and p_{eq} is the equilibrium pressure (Mikulčić et al., 2012).

$$\frac{dm_j}{dt} = M_j \vartheta_j k_D \left(p_{eq} - p_{CO_2}\right) A_{sp} A_{eff} \tag{23}$$

$$k_D = 1.22 \times 10^{-5} \exp\left(-\frac{4026}{T_p}\right) \tag{24}$$

$$p_{eq} = 4.192 \times 10^{12} \exp\left(-\frac{20474}{T_p}\right) \tag{25}$$

3. SYSTEM DESCRIPTION

The designed FB reactor, which has a bottom cross section area of 0.286 m² and a total height of 1.880 m, is shown in Fig. 2. This geometry corresponds to the 'Electrically heated calciner' shown in Fig. 1. The top cross section is cylindrical, and a transition piece connects these two sections, as shown in Fig. 2. Based on the design calculations the number of required electrically heated cylinders is 17, and each cylinder has a length of 0.65 m. The cylinders are arranged as shown in Fig. 2, and the bed height before expansion is about the same as the heigh level of the upper cylinder row (0.61 m). Raw meal is injected via rectangular inlets at the reactor sidewalls, below the first row of the hot cylinders.

The designed electrified calciner has two main sections. In the dense mixing section, at the bottom, fine raw meal particles are mixed with coarse CaO particles. The latter are easily fluidized and also act as a thermal reservoir for efficient heat transfer to the fine meal particles. The hot cylinders, which are electrically heated, heat up both the coarse particles and the raw meal. The fine particles are calcined mainly in this dense section of the FB.

The CO_2 resulting from the calcination and the injected fluidization gas is meant to entrain the calcined meal but leave the coarse particles in the dense bed. Hence, this upper dilute section is called the segregation section.

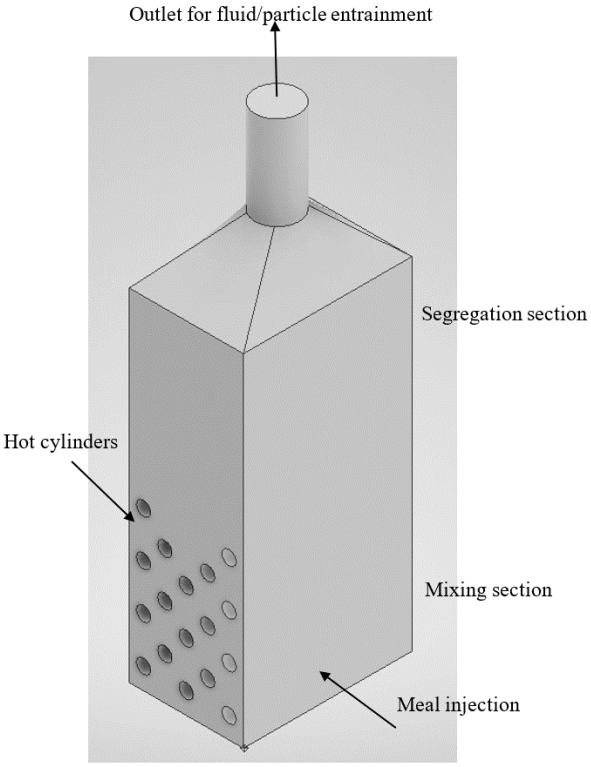

Fig. 2. The designed reactor geometry.

4. MODELLING AND SIMULATION

The designed reactor is modeled and investigated using the commercial software Barracuda, version 21.1.1.

The geometry of the modeled reactor is shown in Fig. 2. The simulation is done in 3D and is dynamic (time dependent). It includes flow particle interactions, $CaCO_3$ decomposition and heat transfer between fluid and particles, between wall and particles and between fluid and wall.

A uniform grid was made in Barracuda as uniform cells will help reaching a stable and efficient simulation (Barracuda-Virtual-Reactor, 2022).

As a grid independence test, the pressure drop in the reactor was compared for four different meshes, having 54000, 130680, 192510 and 250767 cells, respectively. The last three meshes have less than 0.46 % difference in the result. The mesh with 192510 cells was finally selected as it should be fine enough for ensuring accuracy and coarse enough for not requiring too much calculation time. The final mesh is shown in Fig. 3. The design basis values are listed in Table 1. The particle size distributions of the coarse and fine particles are shown in Fig. 4.

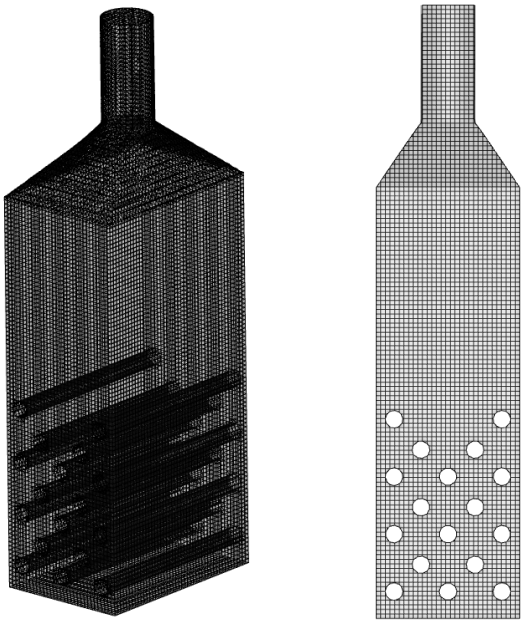

(a) 3D mesh (b) Mesh in the mid plane

Fig. 3. Mesh of the reactor (a) 3-dimensional, (b) The mid plane.

Table 1: Design basis values

Parameter	Description	Value	Unit
w_{CaCO_3}	Weight fraction of $CaCO_3$ in the raw meal	0.77	-
η	Degree of calcination	0.94	-
T_{in,CO_2}	Inlet temperature of fluidization gas	920	°C
T_{coarse}	Initial temperature of coarse particle	920	°C
$\dot{E}$	Electrical energy input	100	kW
U	Overall heat transfer coefficient	0.3	kJ/(m²·K)
D_{cyl}	Cylinder diameter	0.055	m
D_{top}	Diameter at the reactor exit	0.170	m
u_{out}	Required entrainment velocity	1.7	m/s
ρ_{coarse}	Envelope density of coarse particles	1600	kg/m³
ρ_{rm}	Envelope density of raw meal	2700	kg/m³

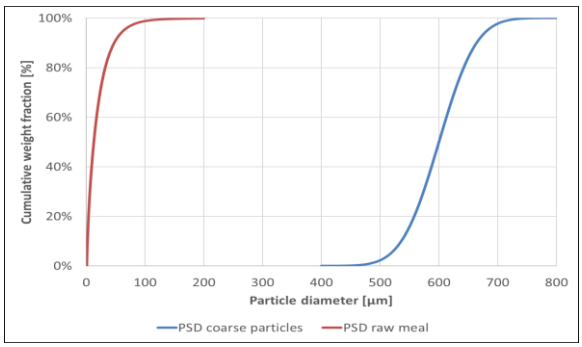

Fig. 4. Particle size distribution of coarse and fine particles.

4.1 Simulation setup

The initial timestep was set to 0.001 s. However, to maintain the accuracy, stability and calculation speed, the simulator checks the Courant number to stay in the preferred range ($0.8 < CFL < 1.5$), and it adjusts the time step if needed (Barracuda-Virtual-Reactor, 2022). The simulation data was saved each 0.1 s.

To solve the fluid governing equations, an LES model was selected as the turbulence model. The conversion criteria were set to10^{-6} for the pressure and energy calculations, 10^{-7} for the volume and velocity and 10^{-9} the radiation. These values were suggested in Barracuda (Barracuda-Virtual-Reactor, 2022).

4.2 Boundary conditions and case definitions

Seven different cases were defined, see Table 2. In all cases, the pressure at the outlet was set to 1 atm, a meal feed rate of 169 kg/h was applied, and the fluidization gas temperature was set to 920 °C. The initial temperature was set to 920 °C for both fluid and coarse particles in all cases. The initial height of the bed (before expansion) was 0.61 m.

Table 2. Case definitions

Case	$T_{in,rm}$ [°C]	T_{cyl} [°C]	u_F [m/s]
1	20	1050	0.3
2	20	1150	0.3
3	720	1150	0.3
4	850	1050	0.3
5	850	1100	0.3
6	850	1100	0.4
7	850	1100	0.8

4.3 Calcination degree, particle entrainment and heat transfer coefficient

The calcination degree, the fine particle entrainment, the coarse particle entrainment, and the heat overall heat transfer coefficient are four important factors in the evaluation of the FB performance.

To calculate the calcination degree, a flux plane is defined at the outlet of the reactor, and the fluid mass flow rate exiting the reactor ($\dot{m}_{CO_2,out}$) is found from the simulation results. This amount includes both the fluidization CO_2 ($\dot{m}_{CO_2,in}$) and the CO_2 due to reaction. From design calculations it is known how much CO_2 is injected and how much CO_2 should be produced ($\dot{m}_{CO_2,prod,design}$). So, the calculation of calcination degree is as follows:

$$\eta_{cal} = \frac{\dot{m}_{CO_2,out} - \dot{m}_{CO_2,in}}{\dot{m}_{CO_2,prod,design}} \times 100\ \% \quad (26)$$

The flow rate of fine particles across the exit flux plane can be compared with the feed rate of particles. Sometime after

feeding is started, a pseudo-steady state should be reached where there is a balance between the inlet and outlet of fine particles (compensated for the calcination degree), cf. equations (4)-(8).

The flow rate of coarse particles across the exit flux plane should ideally be zero, but some entrainment is likely. The loss rate must be compensated by a make-up stream of coarse particles, and this make-up stream should be low compared with the meal feed rate. A small make-up may be acceptable.

The overall heat transfer coefficient can also be calculated based on the simulation results. This value can then later be verified in experiments. The calculation of this coefficient can be made reusing the energy balance in equations (1)-(3), but now utilizing that the area is known (from the design calculations) and treating the U value as an unknown.

5. RESULT AND DISCUSSION

All the simulations are continued until a pseudo-steady state has been reached, i.e., when the outlet mass flow rate remains steady. The results show that the pseudo-steady state is reached before 45 seconds for all the simulated cases. The avoided CO_2 emissions, when compared with a coal-fired cement kiln system, have been calculated based on typical operational settings for a full-scale system. There is a strong correlation to calcination degree, and the reduction varies from 44 % to 79 %, the latter being a very significant reduction. An example is shown in Fig. 5 for Case 2. Also, by injection of the raw meal in a narrow long injection area below the first row of hot cylinders a good mixing is reached in all the simulation cases. As an example, the distribution of injected raw meal particles just after 3 seconds is shown in Fig. 6 . It shows that they are well distributed in the reactor. The particle volume fraction at the 45th second after reaching the pseudo steady state condition is shown in Fig. 7 which also reveals a good mixing condition.

The calcination degree in Case 2 can be calculated to 69 % using equation (23), noting that the mass flow of produced CO_2 based on design for cases 1-5 is 57 kg/h.

The effect of different operating conditions on the calcination degree is shown in Fig. 8. When the feed is not preheated (20 °C), a big part of the energy supply is spent on heating the raw meal (Case 1 and 2), and when the heater temperature is low (1050 °C, as in Case 1) the driving force for heat transfer is low, so, the calcination degree becomes low. The result is 50 % for Case 1 and 69 % for Case 2. Moreover, when the calcination degree is very low, such as in Case 1, the fine particles will not be properly entrained, and the system will not work.

Using a high cylinder temperature (1150 °C) and feeding raw meal preheated to 720 °C (Case 3) significantly increases the calcination degree from 69 % to 90 %, which is a very good value for stable production.

If the heater temperature is kept at 1050 °C and the meal is preheated to 850 °C (Case 4), the calcination degree reaches 81 %. However, if instead the heater temperature is increased to 1150 °C and the meal is preheated to 720 °C (Case 5), the calcination degree reaches 90 %, i.e., the same as in Case 3. This shows the importance of being able to operate a high heater temperature in the bed.

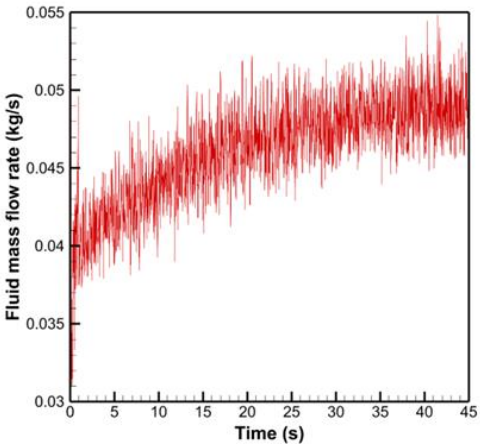

Fig. 5. Gas mass flow rate exiting the reactor (Case 2).

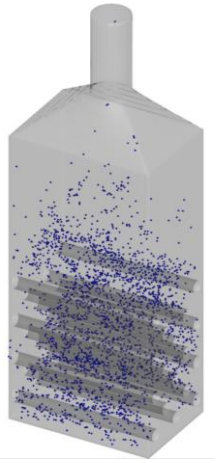

Fig. 6. The raw meal distribution after 3 seconds.

Apart from the calcination degree, particle entrainment is of great importance. The particle entrainment for two cases with low (Case 2) and high calcination degree (Case 3) is shown in Figs. 9 and 10, respectively.

In both cases, there is a very low amount of particle entrainment before 27 s. After this time, it appears that the reaction has reached steady state as the fluid flow rate exiting the reactor stopped increasing and only resonating around a specific value (Fig. 5). Also, the time integrated particle mass (Fig. 9) is increasing with a constant slope, showing that pseudo steady conditions is reached.

To check the mass balance and ensure that the pseudo steady condition is reached, the mass flow rate of raw meal injection should be equal to sum of the mass flow rate of fine particle entrainment and the produced CO_2 exiting the reactor. The total amount of fine particles injected into the reactor was 169 kg/h. Calculating from the 28th to the 45th second, the slope of entrainment of fine particles in Case 2 is 133 kg/h. The fluid mass flow rate exiting the reactor shows 175 kg/h, where 139 kg/h was the injected gas, so the production rate of CO_2 is 36

kg/h. The sum of 133 and 36 is 169, so there is a balance in the mass. Hence, the fine particles are entrained as expected.

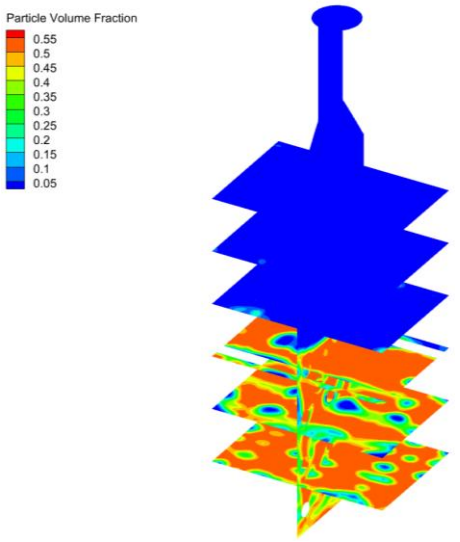

Fig. 7. Particle volume fraction in the 45th second (Case 2).

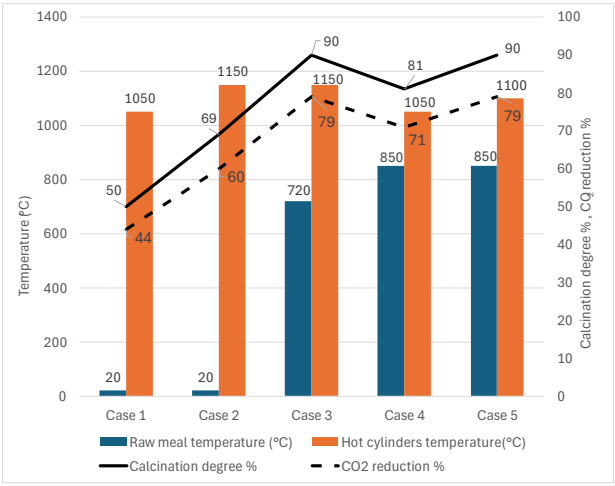

Fig. 8. Calcination degree and CO_2 reduction for cases 1-5.

In Case 2, a cold raw meal (20 °C) is injected, whereas in Case 3, the meal is preheated (720 °C) as it would be in an industrial system. The entrainment of coarse particles is about 0.9 % of the meal feed rate in Case 2, and about 2.4 % in Case 3. The entrainment of coarse particles is higher in the latter case due to the higher calcination degree and thereby a higher flow rate gas leaving the reactor. Anyway, both values are quite low, indicating an acceptable reactor design.

The fluidization velocity has a significant effect on the particle residence time in the bed and the entrainment of particles. Figure 11 shows that increasing the fluidization velocity from 0.3 m/s to 0.4 m/s reduces the calcination degree from 90 % to 80 %. The reason might be the residence time of the particles in the bed, which is reduced from 24.5 s to 20 s.

Increasing the velocity to 0.8 m/s gives a calcination degree of only 56 % and the residence time is only 5 s. However, this is not a stable value as the coarse particles are entrained from the bed, as shown in Figure 12. The bed will be emptied of coarse particles in less than an hour, so operating at such a high velocity is not feasible.

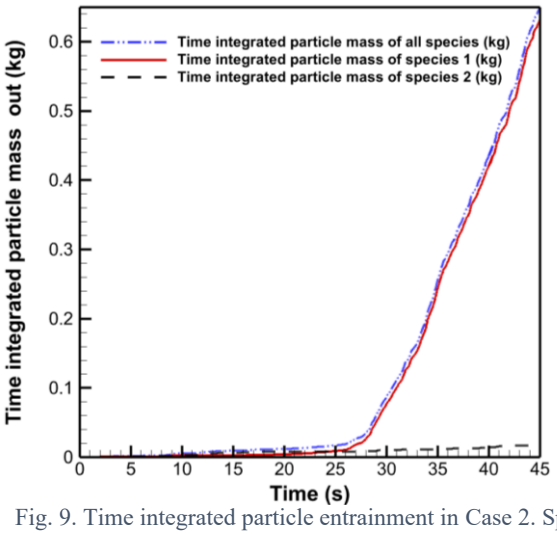

Fig. 9. Time integrated particle entrainment in Case 2. Species 1 is fine particles and species 2 is coarse particles.

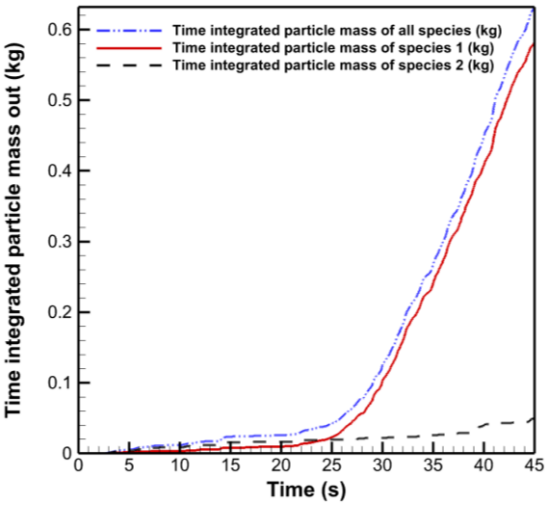

Fig. 10. Time integrated particle entrainment in Case 3. Species 1 is fine particles and species 2 is coarse particles.

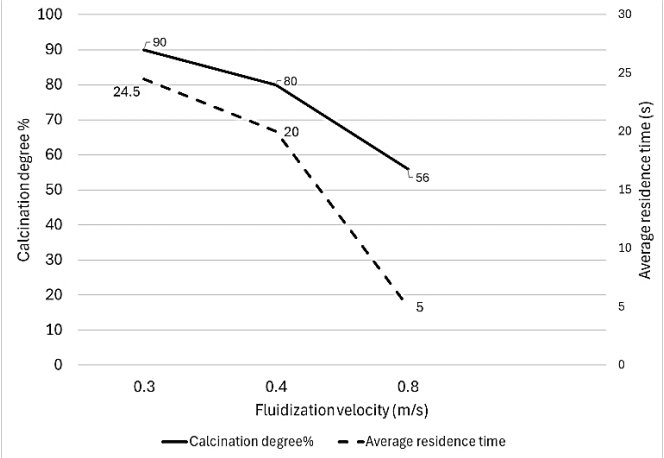

Fig. 11. The effect of fluidization velocity on calcination degree and particle residence time (Cases 5, 6 and 7).

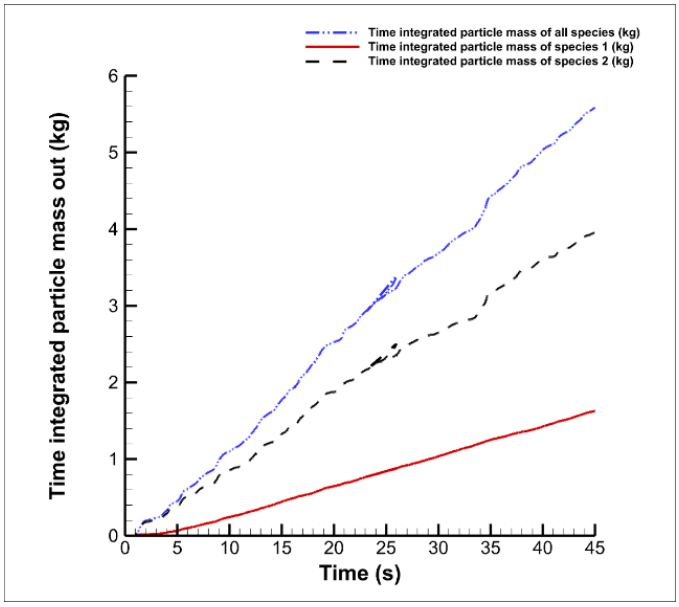

Fig. 12. Time integrated particle entrainment at a fluidization velocity of 0.8 m/s.

6. CONCLUSIONS

The CPFD results indicate that keeping the fluidization velocity constant but increasing the temperature of hot cylinders in the bed and or preheating the meal before injection can significantly increase the calcination degree. Moreover, keeping the temperatures constant but changing the fluidization velocity can significantly affect the calcination degree and the particle entrainment. Increasing the fluidization velocity to 0.8 m/s would give entrainment of all particles, whereas a fluidization velocity of 0.3 m/s works well for the designed reactor. The entrainment of coarse particles is in the range 1-2 % of the meal feed rate, which can be seen as an acceptable value for large-scale production. A high calcination degree of 90 % was reached when the meal was preheated, whereas no meal preheating gave a calcination degree of only 50%, which is due to more of the supplied energy being spent on heating the meal. At 90 % calcination, the resulting CO_2 reduction, compared to a coal-fired kiln system, is 79 %. The average residence time of the fine particles in the dense bed section after reaching the pseudo steady state condition was found to be in the range 24-26 s in five different cases. There was proper fluidization and good mixing of fine and coarse particles in all cases. All in all, calcination of raw meal in the designed electrified fluidized bed calciner appears to be feasible when the gas velocity in the reactor is kept within the specified operational limits.

ACKNOWLEDGEMENTS

This study was done to support the project “Electrification of High Temperature and Flexible Technologies for Transforming Cement, Lime and Pulp Industry” (ELECTRA). University of South-Eastern Norway and Heidelberg Materials are two of the participants of this project, which has received funding from the European Union’s Horizon Europe research and innovation program under Grant Agreement No 101138392.

REFERENCES

Barracuda-Virtual-Reactor (2022). Barracuda Virtual Reactor version: 21.1.1 User Manual. Last updated on Feb 07, 2022. ed. Dupont, C. and Oberthür, S. (2015). The European Union. *Research handbook on climate governance*, 224-236.

Geldart, D. (1973). Types of gas fluidization. *Powder Technology,* 7, 285-292.

IEA (2020). *International Energy Agency, Paris, France, 2020*.

IEA (2018). *Low-Carbon Transition in the Cement Industry*, IEA.

Jacob, R. (2023). *CO_2 capture through electrified calcination in cement clinker production.* Ph.D dissertation, University of South-Eastern Norway.

Jacob, R., Moldestad, B., and Tokheim, L.-A. (2022). *Fluidization of Fine Calciner Raw Meal Particles by mixing with coarser Inert Particles – Experiments and CPFD Simulations*.

Jacob, R. and Tokheim, L.-A. (2023). CPFD simulation of an electrically heated fluidized bed calciner with binary particles. *Energy Conversion and Management: X,* 20, 100444.

Kim, J. H., Bae, J. W., Nam, J., Kim, S. D., Choi, J.-H., and Lee, D. H. (2014). Entrainment of Geldart C particles in fluidized beds with binary particles. *Korean Journal of Chemical Engineering,* 31, 2094-2100.

Mikulčić, H., von Berg, E., Vujanović, M., Priesching, P., Perković, L., Tatschl, R., and Duić, N. (2012). Numerical modelling of calcination reaction mechanism for cement production. *Chemical Engineering Science,* 69, 607-615.

Nikolakopoulos, A., Steriotis, T., Charalampopoulou, G., Karagiannakis, G., Dimitrakis, D., Michalis, V., and Katsiotis, M. (2024). Reducing carbon emissions in cement production through solarization of the calcination process and thermochemical energy storage. *Computers & Chemical Engineering,* 180, 108506.

Samani, N. A., Jayarathna, C. K., and Tokheim, L.-A. (2020). CPFD simulation of enhanced cement raw meal fluidization through mixing with coarse, inert particles. *SIMS 61.* Linköping.

Snider, D. M. (2001). An Incompressible Three-Dimensional Multiphase Particle-in-Cell Model for Dense Particle Flows. *Journal of Computational Physics,* 170, 523-549.

Snider, D. M., Clark, S. M., and O'Rourke, P. J. (2011). Eulerian–Lagrangian method for three-dimensional thermal reacting flow with application to coal gasifiers. *Chemical Engineering Science,* 66, 1285-1295.

Tokheim, L.-A., Mathisen, A., Øi, L. E., Jayarathna, C., Eldrup, N., and Gautestad, T. (2019). Combined calcination and CO_2 capture in cement clinker production by use of electrical energy. *TCCS-10.* Trondheim, Norway.